Selected papers presented at the XIII All-Polish Seminar on Mössbauer Spectroscopy (OSSM 24)

Enthalpy of Solution of Rhodium in Iron Studied by ^{57}Fe Mössbauer Spectroscopy

R. Konieczny*, M. Sobota and R. Idczak

Institute of Experimental Physics, University of Wrocław, pl. M. Borna 9, 50-204 Wrocław, Poland

Doi: 10.12693/APhysPolA.146.239 *e-mail: robert.konieczny@uwr.edu.pl

The room temperature Mössbauer spectra of ^{57}Fe were measured for $Fe_{1-x}Rh_x$ solid solutions with x in the range $0.01 \leq x \leq 0.06$. The obtained data were analysed in terms of the binding energy E_b between two rhodium atoms in the studied materials using the extended Hrynkiewicz–Królas model. The extrapolated value of E_b for $x = 0$ was used to compute the enthalpy $H_{\mathrm{Fe-Rh}}$ of solution of Rh in the α-iron matrix. It was found that the enthalpy $H_{\mathrm{Fe-Rh}}$ value is negative and rhodium atoms interact repulsively. The result was compared with the value derived from Miedema's cellular atomic model of alloys.

topics: Mössbauer spectroscopy, hyperfine parameters, binding energy, enthalpy of solution in binary iron alloys

1. Introduction

The ^{57}Fe Mössbauer spectroscopy is a useful tool for studying the interactions of impurity atoms dissolved in iron [1–9]. The technique is especially effective when the impurity neighbours of the Mössbauer probe have a sufficiently large effect on the hyperfine field generated at the probe to yield distinguishable components in the Mössbauer spectrum attributed to different configurations of the probe neighbours. Our recent research [10–14] shows that the technique can also be successfully applied to binary iron systems for which one observes in the Mössbauer spectra a small effect of the hyperfine field generated at the ^{57}Fe probe. These facts are worth noticing because the impurity interactions are simply related to the enthalpy of the solution of the impurity elements in iron [15], and the enthalpy is widely used in developing and testing different models of binary alloys as well as methods for calculating the alloy parameters [16–19]. At the same time, this system may be used as a model system for which, by the *ab initio* calculations, the structural, energetic, thermodynamic, magnetic, and thermoelectric properties were determined [20, 21]. The Mössbauer spectroscopy findings concerning the enthalpy in some cases can be useful for verifying the corresponding experimental data derived from the calorimetric studies [22, 23]. Moreover, the Mössbauer spectroscopy findings in some cases can be impossible to obtain with other methods. It can happen because the calorimetric investigations are performed in relatively high temperatures, above the Curie temperature, at which most of the iron systems are in their γ (fcc) phases, and the influence of magnetic interactions on thermodynamic properties of studied alloys cannot be observed. In turn, the Mössbauer studies provide information about the enthalpy of solution at a relatively low temperature, below the Curie temperature, and in such a case the iron alloys are in the α (bcc) phase.

In this paper, the dilute Fe–Rh iron-based alloys were investigated by ^{57}Fe Mössbauer spectroscopy in order to determine hyperfine interaction parameters, a binding energy of two rhodium atoms and an enthalpy of solution $H_{\mathrm{Fe-Rh}}$ of Rh in α-Fe matrix [9, 22, 24]. To the best of our knowledge, in the available literature, the solution enthalpy values of rhodium in iron have been only predicted from the semi-empirical cellular atomic model of alloys developed by Miedema [18].

2. Experiment and results

2.1. Measurements and sample preparation

The samples of $Fe_{1-x}Rh_x$ alloys, with x in the range between 0.01 and 0.06, were prepared in two steps. The first one was arc melting of appropriate amounts of the high-purity components in an argon

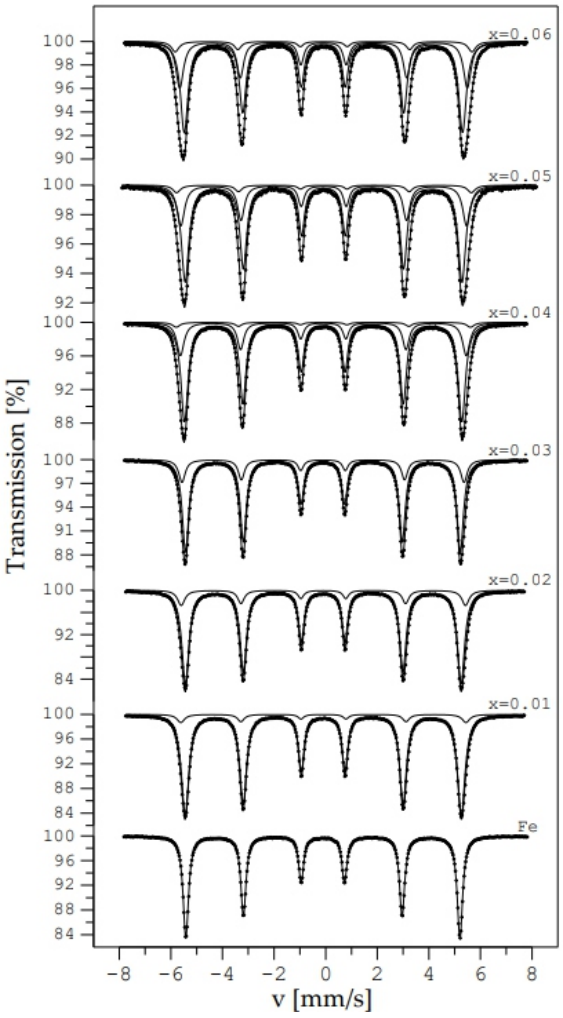

Fig. 1. The room temperature ^{57}Fe Mössbauer spectra for the $Fe_{1-x}Rh_x$ alloys measured just after the melting in an arc furnace.

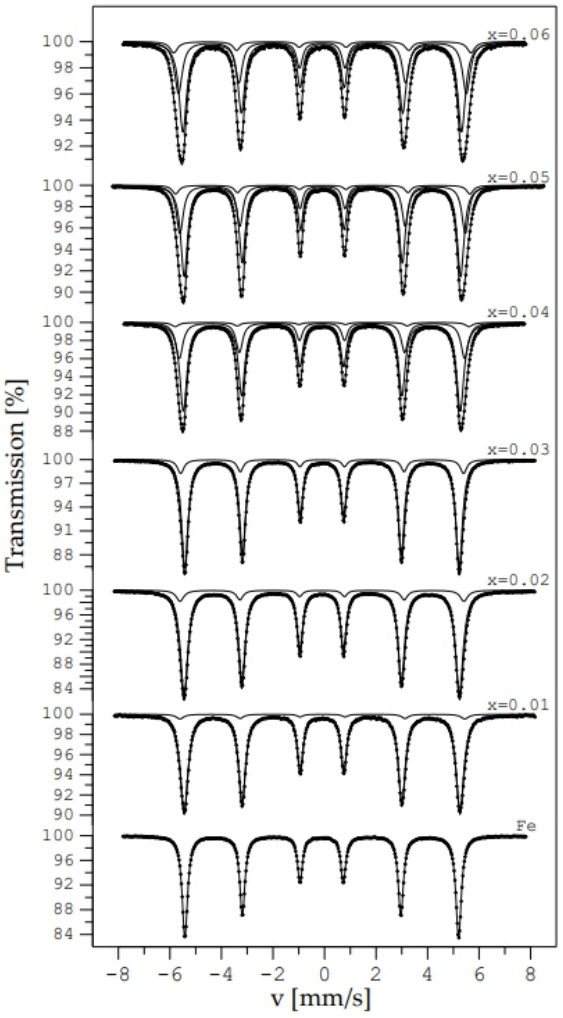

Fig. 2. The ^{57}Fe Mössbauer spectra for the $Fe_{1-x}Rh_x$ alloys measured at room temperature after the annealing process at 1270 K and slow cooling to room temperature.

atmosphere and quick cooling to room temperature. The weight losses during the melting process were below 1%, so it could be assumed that the chemical compositions of the obtained ingots are close to nominal ones. In the second step, the resulting ingots were cold-rolled to the final thickness of about 40 μm. The foils were annealed in the vacuum at 1270 K for 2 h, and after that, they were cooled to room temperature with a cooling rate of about 3 K/min. Under these conditions, diffusion effectively stops at about 700 K [25], so the observed distributions of atoms in the annealed samples should be in the frozen-in state corresponding to 700 K. The room temperature measurements of the ^{57}Fe Mössbauer spectra for each sample were performed twice, before and after the annealing process mentioned above. The spectra were taken in transmission geometry (TMS) by means of a constant-acceleration Mössbauer spectrometer from POLON, Warszawa, using standard source ^{57}Co in Rh of activity 50 mCi with a full width at half maximum (FWHM) of 0.22 mm/s. The ^{57}Co Mössbauer source was manufactured by the RITVERC and supplied by the Eurostandard CZ company.

2.2. Spectra analysis

The measured Mössbauer spectra for Fe–Rh alloys were fitted with a sum of different six-line components corresponding to the various hyperfine fields B at ^{57}Fe nuclei generated by different numbers of Rh and Fe atoms located in the first coordination shell of the probing nuclei. The number of components increased with the atomic concentration of rhodium in the samples. The obtained fits are presented in Figs. 1 and 2.

The fitting procedure was done under the assumption that the influence of n Rh atoms on B as well as the corresponding IS is additive and

TABLE I

The best-fit parameters of the assumed model of the ^{57}Fe Mossbauer spectrum measured for $Fe_{1-x}Rh_x$ alloys. The standard uncertainties for the parameters result from the variance of the fit. Values of the isomer shift IS_0 are reported relative to the corresponding value for α-Fe at room temperature.

x	B_0 [T]	ΔB [T]	IS_0 [mm/s]	ΔIS [mm/s]
0.01	33.17(3)	1.08(6)	0.014(6)	0.016(2)
0.02	33.11(3)	1.03(2)	0.002(5)	0.010(4)
0.03	33.00(2)	1.02(2)	0.011(4)	0.006(2)
0.04	33.30(4)	1.02(2)	0.005(5)	0.006(1)
0.05	33.25(6)	1.07(2)	0.025(5)	0.007(1)
0.06	33.52(5)	1.11(3)	0.018(7)	0.006(1)
x	Γ_{16} [mm/s]	Γ_{25} [mm/s]	Γ_{34} [mm/s]	I_{16}
0.01	0.350(2)	0.317(2)	0.268(3)	2.32(4)
0.02	0.352(2)	0.309(2)	0.263(2)	2.35(3)
0.03	0.302(1)	0.277(1)	0.247(2)	2.41(3)
0.04	0.339(2)	0.311(2)	0.277(2)	2.48(3)
0.05	0.349(2)	0.291(2)	0.257(2)	2.59(3)
0.06	0.359(3)	0.326(3)	0.289(3)	2.50(4)

independent of the atom positions in the neighbourhood of the nuclear probe, so the relationship between B, IS, and n can be written as follows

$$B(n) = B_0 + n\Delta B,$$
$$IS(n) = IS_0 + n\Delta IS, \tag{1}$$

where B_0, ΔB, IS_0, and ΔIS are fitted parameters; B_0 (ΔB) and IS_0 (ΔIS) stand for the change in B and IS with zero (one) rhodium atom in the first coordination shell of the Mössbauer probe. Simultaneously, the quadruple shift QS of a subspectrum is a free parameter and is close to zero. Moreover, it was assumed that the shape of each line is Lorentzian and the three linewidths Γ_{16}, Γ_{25}, and Γ_{34} as well as the two line area ratios I_{16}/I_{34} and I_{25}/I_{34} are the same for all six-line components of the given spectrum.

In many cases, the above assumptions are enough to obtain reasonable results. However, in studied alloys, rhodium neighbours of the Mössbauer probe have a very small effect on the hyperfine field generated at the probe, so proper decomposition of the Mössbauer spectra to several components is impossible without additional assumptions about the parameters of the components. For a successful analysis of these spectra, we used two series of data. The first one is for samples frozen in a high-temperature state just after melting, and the second one is for samples after annealing at 1270 K for 2 h. The as-obtained samples can be treated as disorder alloys, in which the probability of the existence of n rhodium atoms among all N atoms located in the first coordination shell of the ^{57}Fe probe is given by the binomial distribution

$$p_n = \frac{N!}{(N-n)!n!}\, x^n (1-x)^{N-n}. \tag{2}$$

We have accepted that $N = 8$ for bcc structures of the studied Fe–Rh alloys. It is worth noting that the fits obtained under these assumptions are quite good. Moreover, the found values of the best-fit parameters displayed in Table I differ essentially from the corresponding data given in the literature, e.g., in [26–29].

TABLE II

The binding energy E_b between a pair of Rh atoms in $Fe_{1-x}Rh_x$ alloys deduced from the ^{57}Fe Mössbauer spectra. The standard uncertainties for c_1 and c_2 result from the variance of the fit of the assumed model to the spectra measured.

x	c_1	c_2	p_1	p_2	E_b [eV]
0.01	0.0456(4)	–	0.0746	0.0026	–
0.02	0.0975(3)	–	0.1389	0.0099	–
0.03	0.1135(2)	–	0.1939	0.0210	–
0.04	0.2808(4)	0.0326(3)	0.2405	0.0351	0.0167(9)
0.05	0.3255(3)	0.0584(2)	0.2793	0.0515	0.0020(4)
0.06	0.3392(6)	0.0726(4)	0.3113	0.0695	0.0034(5)

2.3. The binding energy E_b of two rhodium atoms in the iron matrix

The obtained values of hyperfine parameters of the best-fit model were used to determine relative shares c_1 and c_2 of the second and third components of each spectrum. The components are related to the existence of one and two rhodium atoms in the first coordination shell of the ^{57}Fe probe. Assuming that the Lamb–Mössbauer factor is independent of the configuration of atoms in the surroundings of the Mössbauer probe, the c_1 and c_2 values represent the intensities of the components mentioned above. The results are presented in Table II.

To calculate the binding energy E_b for pairs of Rh atoms, c_1 and c_2 values of spectrum components for annealed samples were used. The calculations E_b were performed on the basis of the modified Hrynkiewicz–Królas formula [1]

$$E_b = -k_{\mathrm{B}} T_d \ln\left[\left(1+\frac{2c_2}{c_1}\right)\frac{c_2}{c_1}\left(1+\frac{2p_2}{p_1}\right)^{-1}\left(\frac{p_2}{p_1}\right)^{-1}\right]. \tag{3}$$

In the above equation, k_{B} is the Boltzmann constant, $T_d = 700(11)$ K denotes the freezing temperature for the atomic distribution in annealed Fe–Rh alloys, whereas p_1 and p_2 are probabilities of the existence of one and two rhodium atoms located in the first coordination shell of the ^{57}Fe probe, given by

TABLE III

The enthalpy $H_{\mathrm{Fe-Rh}}$ [eV/atom] of solution of rhodium in iron.

	Miedema's model [18]	This work (α-Fe)
$H_{\mathrm{Fe-Rh}}$ [eV/atom]	−0.232	−0.164(40)

the binomial distribution. Computed E_b values are presented in Table II. Positive values of the binding energy for all studied samples suggest that interaction between two rhodium atoms in the iron matrix is repulsive.

2.4. Enthalpy of solution of rhodium in iron

In the next step, we found the extrapolated value of the binding energy E_b for $x = 0$, using the E_b values derived from data for the samples with rhodium. The result is $E_b(0) = 0.041(10)$ eV. The obtained $E_b(0)$ value was used to computate an enthalpy $H_{\mathrm{Fe-Rh}}$ of the solution of Rh in Fe. The calculations were performed on the basis of the Królas model [15] for the binding energy according to which

$$H_{\mathrm{Fe-Rh}} = -\frac{zE_b(0)}{2}, \tag{4}$$

where z is the coordination number of the crystalline lattice ($z = 8$ for α-Fe). The result is displayed in Table III, together with the value resulting from Miedema's model of alloys [18]. According to the model

$$H_{\mathrm{Fe-Rh}} = \frac{2V_{\mathrm{Rh}}^{2/3}\left[-P(\Delta\varphi)^2+Q(\Delta n^{1/3})^2-R\right]}{(n_{\mathrm{Fe}}^{-1/3}+n_{\mathrm{Rh}}^{-1/3})}, \tag{5}$$

where V_{Rh} is the atomic volume of Rh, φ is the electronegativity, $n^{1/3}$ is the cubic root of the electron density at the boundary of bulk Wigner–Seitz cells, and Δ denotes the differences in a given parameter for Fe and Rh. The coefficients P, Q, and R are empirical constants; $PN_A = 14.1$ kJ/(V^2 (d.u.)$^{1/3}$ cm^2); $Q/P = 9.4$ V^2/(d.u.)$^{2/3}$ and $R = 0$ for alloys of two transition metals; N_{A} is the Avogadro's number; d.u. is about 4.6×10^{22} electrons per cm^3; $\varphi_{\mathrm{Rh}} = 5.40$ V; $\varphi_{\mathrm{Fe}} = 4.93$ V; $n_{\mathrm{Rh}} = 5.45$ d.u.; $n_{\mathrm{Fe}} = 5.55$ d.u.; $V_{\mathrm{Rh}} = 8.3$ cm^3/mol; $V_{\mathrm{Fe}} = 7.1$ cm^3/mol.

3. Conclusions

The results obtained in this study give rise to the following conclusions.

The obtained values of binding energy between two rhodium atoms in Fe–Rh alloys suggest that interaction between rhodium atoms in the studied materials is repulsive.

The obtained value of enthalpy $H_{\mathrm{Fe-Rh}}$ of solution of Rh in α-Fe is 0.164(40) eV/atom and it is worth noting that the $H_{\mathrm{Fe-Rh}}$ value calculated using Miedema's cellular atomic model of alloys is in good agreement with it. According to our knowledge, this thermodynamic parameter was estimated experimentally for the first time for the Fe–Rh system in α (bcc) phase with atomic distributions corresponding to a temperature of about 700 K, below Curie temperature.

References

[1] J. Chojcan, *J. Alloys Compd.* **264**, 50 (1998).

[2] J. Chojcan, *Hyperfine Interact.* **156/157**, 523 (2004).

[3] E. Jartych, *J. Magn. Magn. Mater.* **265**, 176 (2003).

[4] V.V. Ovchinnikov, B.Yu. Goloborodsky, N.V. Gushina, V.A. Semionkin, E. Wieser, *Appl. Phys. A* **83**, 83 (2006).

[5] Y. Yoshida, F. Langmayr, P. Fratzl, G. Vogl, *Phys. Rev. B* **39**, 6395 (1989).

[6] R. Idczak, R. Konieczny, J. Chojcan, *Solid State Commun.* **159**, 22 (2013).

[7] R. Idczak, B. Kaśków, R. Konieczny, J. Chojcan, *Physica B Condens. Matter* **577**, 411794 (2020).

[8] J. Chojcan, R. Konieczny, A. Ostrasz, R. Idczak *Hyperfine Interact.* **196**, 377 (2010).

[9] R. Konieczny, R. Idczak, J. Chojcan, *Nukleonika* **60**, 75 (2015).

[10] R. Idczak, R. Konieczny, Ż. Konieczna, J. Chojcan, *Acta Phys. Pol. A* **119**, 37 (2011).

[11] R. Konieczny, R. Idczak, *Nukleonika* **62**, 9 (2017).

[12] R. Konieczny, J. Chojcan, *Acta Phys. Pol. A* **134**, 1053 (2018).

[13] R. Konieczny, R. Idczak, J. Chojcan, *Acta Phys. Pol. A* **131**, 255 (2017).

[14] R. Idczak, R. Konieczny, J. Chojcan, *Acta Phys. Pol. A* **129**, 367 (2016).

[15] K. Królas, *Phys. Lett. A* **85**, 107 (1981).

[16] G. Bonny, R.C. Pasianot, L. Malerba, A. Caro, P. Olsson, M.Yu. Lavrentiev, *J. Nucl. Mater.* **385**, 268 (2009).

[17] R. Boom, F.R. De Boer, A.K. Niessen, A.R. Miedema, *Physica B + C* **115**, 285 (1983).

[18] A.R. Miedema, *Physica B* **182**, 1 (1992).

[19] K. Lejaeghere, S. Cottenier, S. Claessens, M. Waroquier, V. Van Speybroeck, *Phys. Rev. B* **83**, 184201 (2011).

[20] M.J. Jiménez, A.B. Schvval, G.F. Cabeza, *Computat. Mater. Sci.* **172**, 109385 (2019).

[21] E. Valiev, R. Gimaev, V. Zverev, K. Kamilovd, A. Pyatakov, B. Kovalev, A. Tishin, *Intermetallics* **108**, 81 (2019).

[22] R. Hultgren, P.D. Desai, D.T. Hawkins, M. Gleiser, K.K. Kelley, "Selected Values of the Thermodynamic Properties of Binary Alloys", American Society for Metals, Metals Park, Ohio, 1973.

[23] L.J. Swartzendruber, V.P. Itkin, C.B. Alcock, in: *Phase Diagrams of Binary Iron Alloys*, Ed. H. Okamoto, Materials Information Society, Materials Park, Ohio 1993.

[24] A.Z. Hrynkiewicz, K. Królas, *Phys. Rev. B* **28**, 1864 (1983).

[25] T.E. Cranshaw, *J. Phys. Condens. Matter* **1**, 829 (1989).

[26] I. Vincze, I.A. Campbell, *J. Phys. F* **3**, 647 (1973).

[27] G. Shirane, C.W. Chen, P.A. Flinn, R. Nathans, *Phys. Rev.* **131**, 183 (1963).

[28] A. Błachowski, K. Ruebenbauer, J. Żukrowski, *J. Alloys Compd.* **477**, 4 (2009).

[29] A. Błachowski, U.D. Wdowik, *J. Phys. Chem. Solids* **73**, 317 (2012).